SUPPLEMENTAL FIGURES

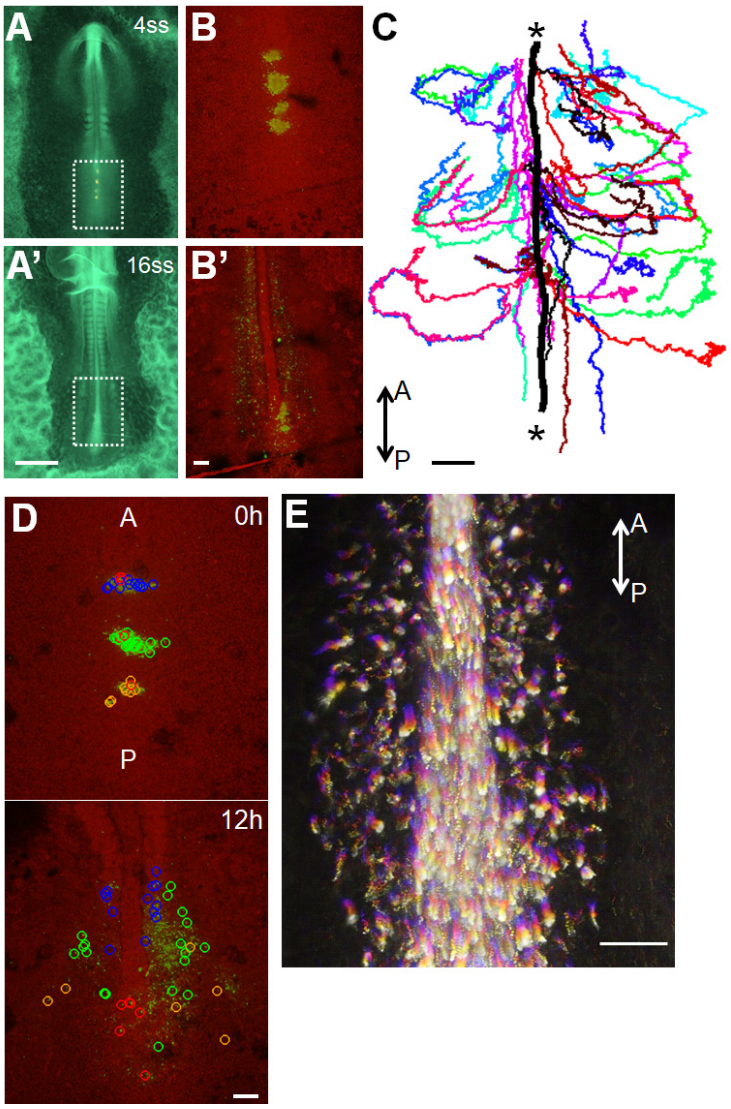

Figure S1. Live imaging and cell tracking in the elongating chicken embryo, related to Figure 1

(A) Examples of live imaging in widefield fluorescence. Whole Tg(CAG:GFP) chicken embryos (ventral view) at indicated somite stages (ss) are shown. Boxes show imaged regions in (B) Scale bar: 1mm.

(B) Examples of confocal cellular live imaging. 3D maximum projections of confocal stacks (ventral view) of the elongating axis are shown. Ubiquitous GFP signal is shown in red, green clusters show DiI labeled sites and cells. These cells were labeled in the PD and many of them later become PSM cells that flank the NC while some remain in the PD (B'). Scale bar: 100μm.

(C) Example of cell tracking. Single cell tracks (n=46) obtained by manual tracking (Movie S1) are plotted over the duration of the movie (~15h). Asterisks mark the trajectory (bold black) of the end of NC/Node area. A, anterior, P, posterior (same below). Scale bar: 100μm.

(D) Fate map of labelled cells colored as different groups posterior to NC. Blue circled cells and some Green circled cells are in the PD at 0h. Red circled cells either are NC progenitors or did not yet exit the midline in the duration of the movie (remaining in the PD). Somites and NC are distinguishable in the top and center of the right panel. Scale bar: 100μm.

(E) Short-term cell movement analysis using high resolution movie (~1h) overlay. Fire color shows progressing of time (colder is earlier). NC cells in the middle show directional posterior movement whereas PSM cells on both sides do not show directional bias indicating short-term random motility. Scale bar: 100μm.

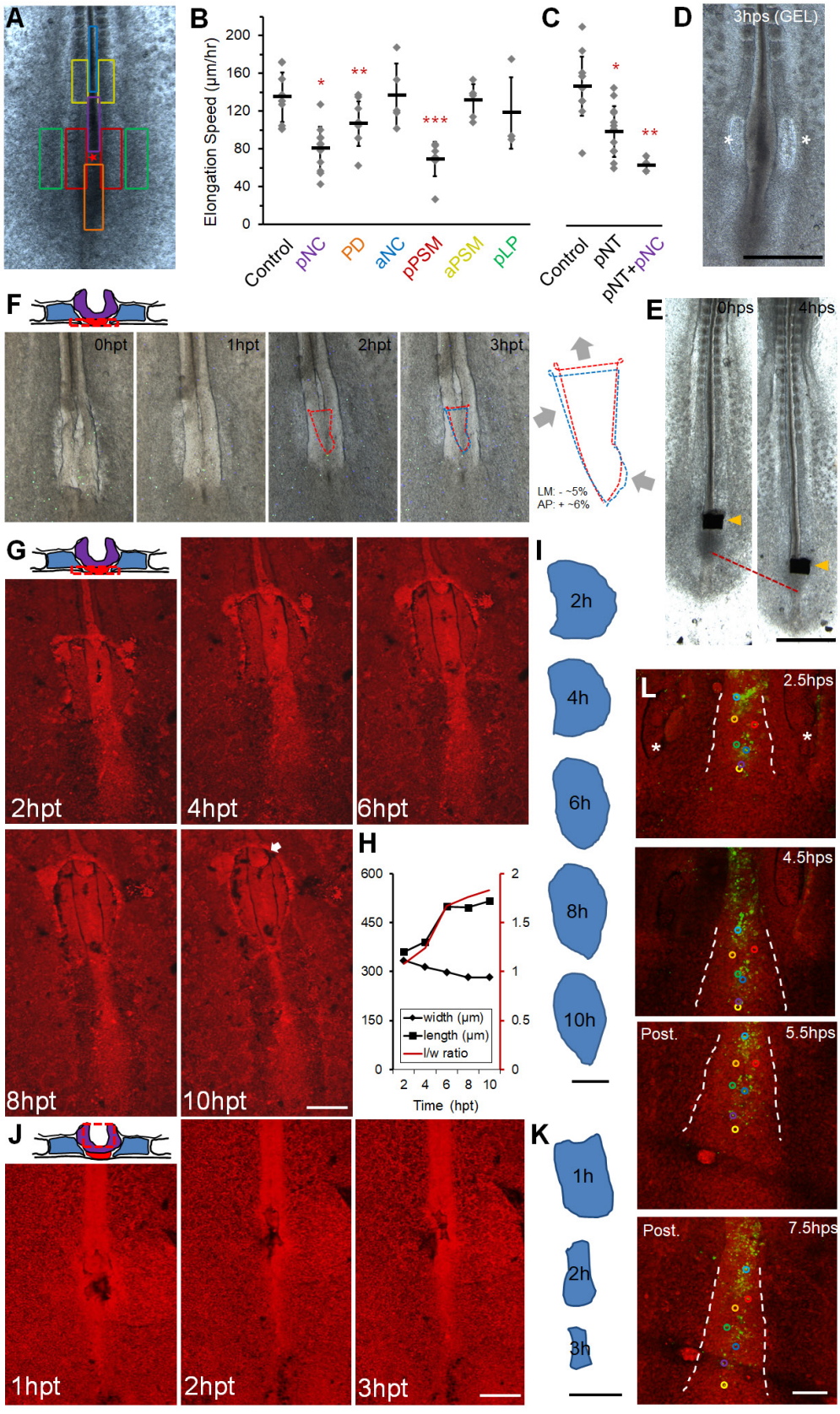
A
B
Elongation Speed (μm/hr)
200
160
120
80
40
0
Control
pNC
PD
aNC
pPSM
aPSM
pLP
C
Control
pNT
pNT+pNC
D
3hps (GEL)
E
0hps
4hps
F
0hpt
1hpt
2hpt
3hpt
LM: - ~5%
AP: + ~6%
G
2hpt
4hpt
6hpt
8hpt
10hpt
H
600
450
300
150
0
2
1.5
1
0.5
0
width (μm)
length (μm)
l/w ratio
2 4 6 8 10
Time (hpt)
I
2h
4h
6h
8h
10h
J
1hpt
2hpt
3hpt
K
1h
2h
3h
L
2.5hps
4.5hps
Post.
5.5hps
Post.
7.5hps

Figure S2. pPSM compresses axial tissues and is important for axial elongation, related to Figure 2

(A-C) Effects of tissue ablation on elongation speed. The embryo image (A) shows different ablation sites (ventral operations) with colors corresponding to elongation speed measurements in (B). (C) shows pNT ablations (dorsal operations) with its own control. Each mark represents an embryo followed over a 6-hour window after surgery. pPSM, pNC, pNT and PD ablations result in significant reduction of elongation speed (asterisks, $p<0.05$, t-tests). aPSM, aNC and pLP (lateral plate) ablations do not ($p>0.05$, t-tests). pNT/pNC double ablation results in a stronger reduction than pNT alone ($p=0.02$, t-test, panel C).

(D) Gel replacement of pPSM. Asterisks, gel implant sites. Widening of the gel flanked portion is observed in 4/4 embryos. Scale bar: 500μm.

(E) Foil insertion between the pNC and PD. The cross-sectional foils are ~200x200μm.

(F) Gel replacement of pNC. Cross-section schematic shows the ablation of pNC from the ventral side. Only endoderm and pNC were ablated, NT is visible through the gel. Slight deformation of the gel can be observed through time. Dashed lines collect five fluorescent beads in the gel to a contour. The beads' relative positions change, tracking gel deformation. The blue contour on the 3hpt (hours-post-transplant) image is identical to the red contour on the 2hpt image. The 3hpt contour (red) is narrower laterally than the 2hpt contour (blue) by an average negative strain in LM of ~5%, and is longer in AP (arrows) by ~6%. Anterior to the top.

(G) Similar to (F) with injected gel. Implant boundary is visible and changes over time. Arrow marks protruding NC from anterior cut site. Scale bar: 200μm.

(H) Quantified shape changes of the gel implant in (G). Length (l) is measured along the midline, width (w) is measured following the widest line perpendicular to the midline. Consistent narrowing was observed in n=7 experiments.

(I) Contours of the gel implant in (G). Scale bar: 200μm.

(J-K) Gel replacement of pNT (dorsal view). Consistent narrowing was observed in n=3 experiments. The gel is likely extruded by the tissue in this case. Scale bars: 200μm.

(L) Tracking of labeled NC cells. In this movie NC cells were labeled with DiI and movement of 7 cells were followed through time (colored circles). White dashed lines mark the lateral boundary of the NC. Asterisks mark pPSM ablation site. As the NC cells pass the ablation site, limited tissue convergence and cell-cell rearrangement are seen. In unperturbed posterior (post.) area, tissue narrowing and medial-lateral cell intercalation are apparent. Scale bar: 100μm.

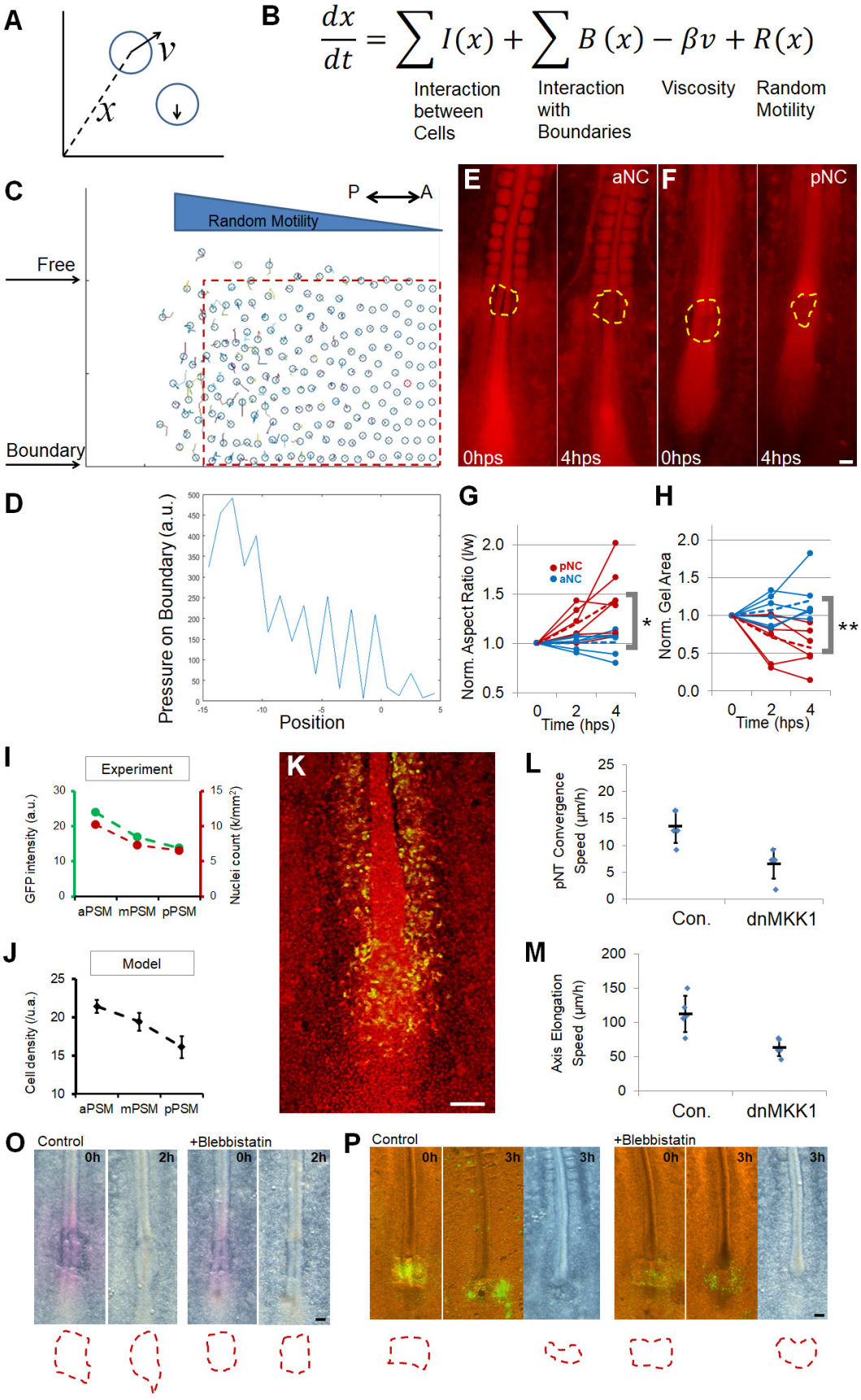
A
v
x
B
$\frac{dx}{dt} = \sum I(x) + \sum B(x) - \beta v + R(x)$
Interaction between Cells
Interaction with Boundaries
Viscosity
Random Motility
C
P ⟷ A
Random Motility
Free
Boundary
D
Pressure on Boundary (a.u.)
Position
E
aNC
0hps
4hps
F
pNC
0hps
4hps
G
Norm. Aspect Ratio (l/w)
pNC
aNC
Time (hps)
*
H
Norm. Gel Area
Time (hps)
**
I
Experiment
GFP intensity (a.u.)
Nuclei count (k/mm²)
aPSM mPSM pPSM
J
Model
Cell density (/u.a.)
aPSM mPSM pPSM
K
L
pNT Convergence Speed (μm/h)
Con.
dnMKK1
M
Axis Elongation Speed (μm/h)
Con.
dnMKK1
O
Control
+Blebbistatin
0h
2h
P
Control
+Blebbistatin
0h
3h

Figure S3. An agent(cell)-based model of co-elongation incorporating the cell motility gradient assumption, related to Figure 3

(A) Cells are defined as circles (with certain radius controlling collision volume) in a plane (tissue space, extracellular matrix). Cells have two main variable attributes: position (x) and velocity (v). Velocity is the time derivative of position.

(B) For each new iteration, a velocity is generated to change the cell's position. The velocity is determined by the forces acting on the cell, which are functions of position and current velocity. The total force is a summary of repulsive interactions between cells (a function of the cell's position and the positions of all other cells) due to collision volume (i.e., cells have volume and cannot occupy the same area), interaction with boundary (such as surface extracellular matrix of the PSM and neighboring tissues such as the lateral plate), effect of viscosity (resistant force against the current movement), and the only active movement component with a random direction and a magnitude as a function of position (i.e., the motility gradient generated by active cell behavior).

(C-D) A random motility gradient causes differential expansion and pressure on confining boundaries. An initial square field of cells (red box) with a gradient of random motility expands over the unconfined (free) space. On a confined boundary, a pressure gradient can be recorded. In the PSM, a similar random motility gradient is observed, and isolated PSM expands preferentially posteriorly. The pressure generated can explain the compression experienced by the pNC/pNT.

(E-F) Deformation of alginate gel implants after surgical ablation of aNC and pNC, respectively. Fluorescent signal (red) is GFP. Yellow dashed lines measure the shape and in-plane area of the gel. Note that the gel volumes are not expected to shrink under compression, the change of area results from gel deformation and flow in the direction perpendicular to the image plane. Scale bar: 100μm.

(G) Normalized gel aspect ratio change. "l" measures the length along AP, "w" along LM. l/w ratios for each sample was normalized by the 0 hps data point. Dashed lines are average ratios. Asterisks mark significant difference between averages at 4 hps (*p=0.018, t-test).

(H) Normalized gel top view area change. Similar to (G), l*w was normalized by 0 hps data point. 4 hps difference **p=0.004, t-test.

(I) Cell density measurement by quantifying GFP intensity (green) or nuclei count using Tg(PGK1:H2B-chFP) quail line (red, Huss et al., 2015) from confocal image z-stacks. a.u., arbitrary units.

(J) Model predictions of cell density along the PSM. Measured areas in the model were adjusted to match measured areas from data. Error bars: ±SD. /u.a., number per unit area.

(K) Electroporation specificity into PSM cells. Image shows a representative embryo electroporated at stage 5 with a membrane-Venus construct into the anterior primitive streak (PD) of a Tg(CAG:GFP) embryo. Confocal image was taken after 24 hours. Positive cells can be seen in the PD and the PSM but not in the midline NC. Scale bar: 100μm.

(L-M) Converging (conv.) speed (±SD) of neural folds towards the midline (L) and elongation speed (±SD) of the axis (M) measured in 3 hours. n=5 for control and n=6 for dnMKK1, $p<0.05$, t-tests.

(O-P) Examples of Blebbistatin treatment on gel deformations (see also Figure 4G). Scale bars: 100μm. (O) pNC gel implants. Pink color is from diffused rhodamine-B mixed with the alginate solution to better show initial gel shape. Blebbistatin treatment delays the smoothening of gel shape and deformation (red contours), suggesting a reduction of tissue force. (P) PD gel implants. Fluorescent beads (green) were mixed with the alginate to better show gel deformation. The beads are loosely trapped in the gel (cannot be washed off but can move). Lateral displacement of beads is seen and is delayed in Blebbistatin treatment. Gel is less compressed from the anterior in Blebbistatin treatment.

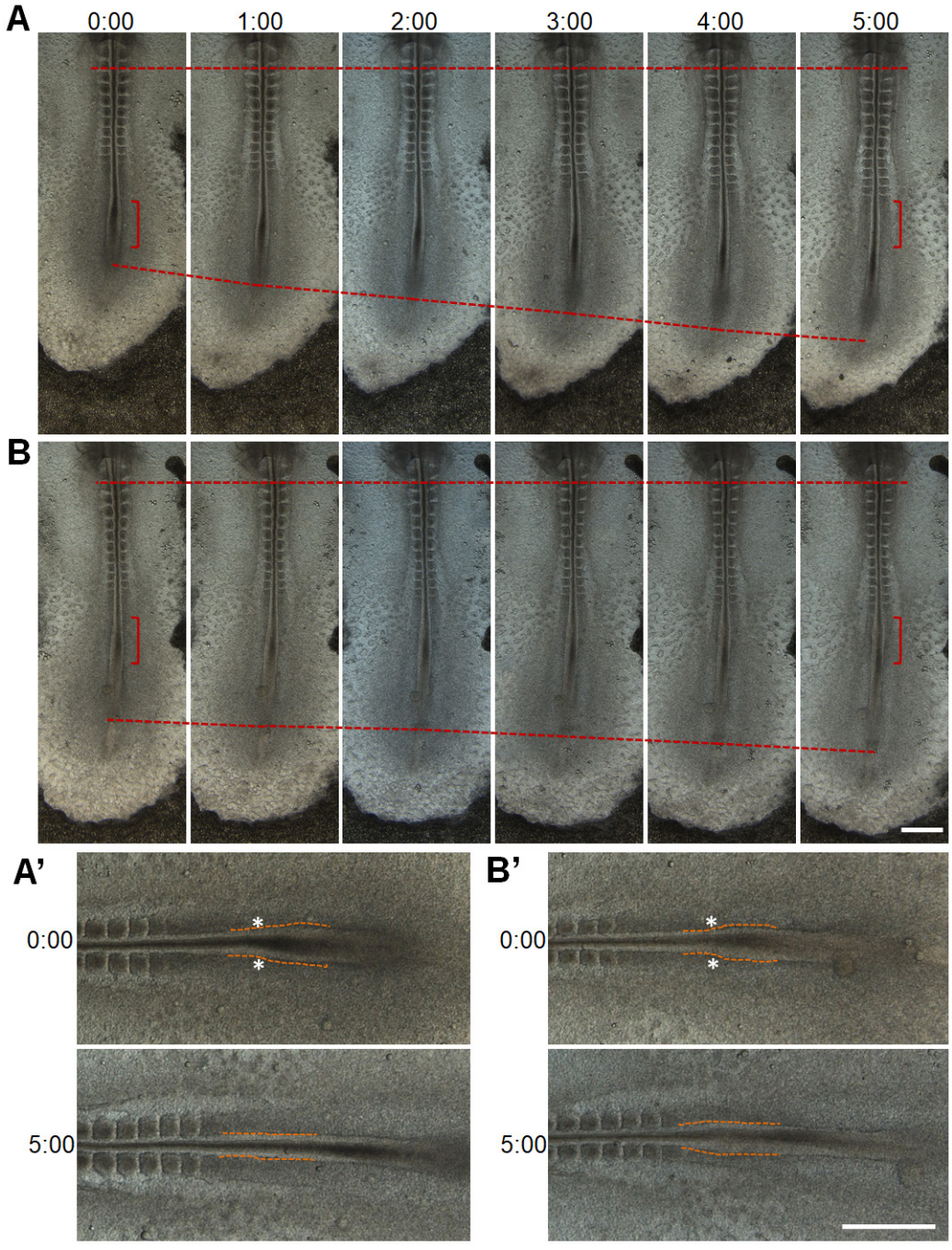
A
0:00
1:00
2:00
3:00
4:00
5:00
B
A'
0:00
5:00
B'
0:00
5:00
C
n= 10 10 5 6 5 6 6 7 n= 6 7
*
***
**
n.s.
****
Elongation Speed (μm/hr)
160
120
80
40
0
PBS (PSM)
WNT5A (PSM)
WNT5A (Node)
WNT10B (PSM)
PD
PD (+WNT5A)
pNC
pNC (+WNT5A)
PBS (NT)
WNT5A (NT)

Figure S4. Elongation and tissue dynamics after WNT5A injection, related to Figure 3

(A-B) Time course of embryos after WNT5A injection at the anterior pPSM level (bracket). Top dashed line marks a fixed somite as the reference, bottom dashed line measures elongation. (A'-B') are enlarged views with dashed lines showing the width of the NT. Asterisks mark the approximate injection location. Scale bars: 500μm.

(C) Elongation speeds after WNT5A injections. The first 4 columns (from left) are injections only, at the injected tissue level indicated in the parenthesis (e.g., PSM, Node). The second 4 columns couple tissue ablation (e.g., PD, pNC) with injections. The NT data (injections only) is shown in a separate panel on the right as the controls were performed separately. Asterisks indicate significant difference ($p<0.05$, t-tests).

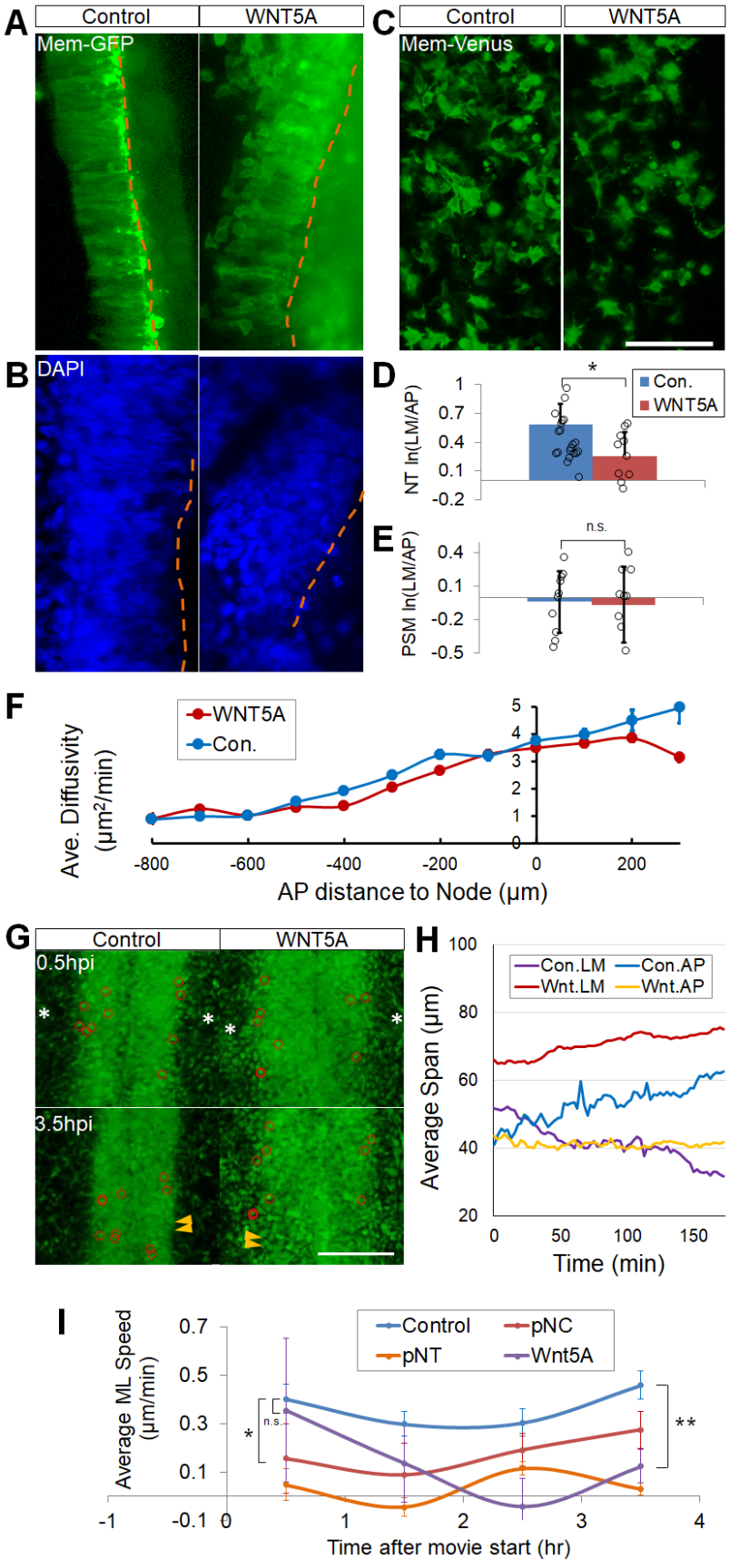
A
Control
WNT5A
Mem-GFP
B
DAPI
C
Control
WNT5A
Mem-Venus
D
NT ln(LM/AP)
1
0.7
0.4
0.1
-0.2
*
Con.
WNT5A
E
PSM ln(LM/AP)
0.4
0.1
-0.2
-0.5
n.s.
F
WNT5A
Con.
Ave. Diffusivity (μm²/min)
5
4
3
2
1
0
-800
-600
-400
-200
0
200
AP distance to Node (μm)
G
Control
WNT5A
0.5hpi
3.5hpi
H
Con.LM
Con.AP
Wnt.LM
Wnt.AP
Average Span (μm)
100
80
60
40
20
0
50
100
150
Time (min)
I
Control
pNC
pNT
Wnt5A
Average ML Speed (μm/min)
0.7
0.5
0.3
0.1
-1
-0.1
0
1
2
3
4
Time after movie start (hr)
*
n.s.
**

Figure S5. pNT cell polarity and dynamics under WNT5A perturbation, related to Figure 3

(A-C) Cell shape analysis using confocal images of cells in live embryos electroporated with a membrane-GFP construct in the NT (A, dorsal view), fixed embryos stained with DAPI in the NT (B, dorsal view), and live embryos electroporated with a membrane-Venus construct in the PSM (C, ventral view), respectively. Yellow dashed lines mark the apical/medial side of the neural fold. Scale bar: 100μm.

(D-E) Quantification of cell shapes by the logarithm of the cell's aspect ratio (lateral-medial length over anterior-posterior length, LM/AP). In (D), NT cells show LM polarization which is reduced after WNT5A injection (n=20, *p=0.004, t-test). In (E), PSM cells show no shape polarization in either condition (n=10, p=0.8, t-test). Similar cell shape changes near the injected area were observed in the NT of all 4 injected embryos but none of 3 controls.

(F) PSM cell motility gradient in a WNT5A injected embryo.

(G) Distribution of tracked cells in a WNT5A injected embryo. The images are 3D maximum projections (dorsal view) of Tg(CAG:GFP) (shown in green) chicken embryos after injection of PBS (control) or WNT5A. Red circles highlighted randomly selected lateral cells at the beginning of the movies at the injected level (marked by asterisks). The pNT is seen in the middle undergoing convergence and elongation through NT cell intercalations. Mesenchymal pPSM cells can be seen flanking the NT. Yellow arrowheads mark the organized vs. disorganized NT areas between control and injected. Scale bars: 100 μm.

(H) Tracking of NT cell intercalation dynamics. 20 cells in each condition were tracked. Average span is calculated using the average position of all cells along either LM or AP direction. Reduction of LM span and a corresponding increase of AP span (as in illustration) indicate cell intercalation.

(I) Timing of slowdown of medial-lateral movement of midline PSM cells after different perturbations. >100 cell movement measurements were taken in each group. Mean speeds ± SD are plotted over time. The WNT5A injection group is similar to control at 0.5hr (n.s., $p>0.05$, t-test) and significantly lower at 3.5hr (**$p<0.05$, t-test). The surgery groups (pNT and pNC) are significantly lower already at 0.5hr (*$p<0.05$, t-tests).

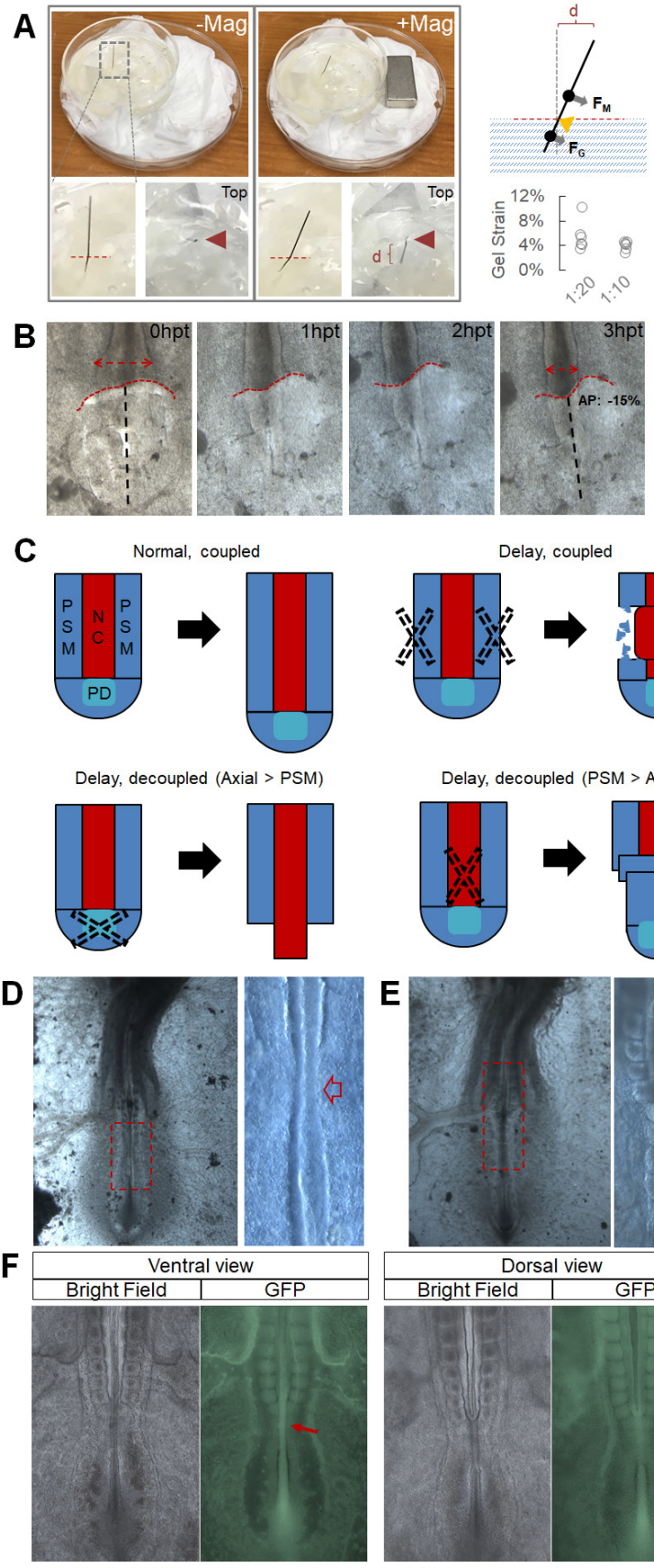
A
-Mag
+Mag
Top
Top
d
F_M
F_G
Gel Strain
12%
8%
4%
0%
1:20
1:10
B
0hpt
1hpt
2hpt
3hpt
AP: -15%
C
Normal, coupled
Delay, coupled
PSM
NC
PSM
PD
Delay, decoupled (Axial > PSM)
Delay, decoupled (PSM > Axial)
D
E
F
Ventral view
Bright Field
GFP
Dorsal view
Bright Field
GFP

Figure S6. Decoupled elongation as a result of breaking the mechanical feedback loop, related to Figure 7

(A) Magnetic pin stress estimation using alginate gels. The left images show the double dish set up used in the experiments. The sample dish (35mm) with the gel or embryo is placed on one end of the 60mm dish that holds the magnet. The steel pin is inserted vertically into a layer of alginate gels on top of the culture medium. Upon magnet addition, the pin rotates and causes a local compression on the gel. The amount of rotation is related to the gel strain. The force from the gel elastic deformation (F_G) and the magnetic attraction force on the pin (F_M) produce torques that balance to determine the rotation angle. The gels were made with indicated volume ratios (1:20 and 1:10) by mixing 5% (w/v) calcium chloride solution with 1% (w/v) alginic acid sodium solution. Given the observed strains on these gels that are much stiffer than the PD tissue, the estimated stress produced by the pin on the interface point is estimated to be much higher than the endogenous axial push (compare to [B]).

(B) Gel implant to replace the progenitor domain (PD). Double headed arrows show the narrowing of the NT. Red dashed lines show the outline of the gel in contact with pNC and pPSM. Here NC becomes longer than PSM as the gel deforms to a heart shape. The dark dashed lines measure a change of the gel length in AP at the midline by ~15%. The gel is made by 1:40 mixing of 5% (w/v) calcium chloride solution with 1% (w/v) alginic acid sodium solution.

(C) Summary illustration of microsurgery ablations that impact elongation rate. pPSM ablation causes a local delay but does not disrupt coupling. PD ablation results in longer axial tissues and axial ablation results in longer and centered PSM.

(D) Left and right PSM merged at the site where pNC was ablated and elongation continued in the long term (>15 hours-post-surgery). Right panel is a zoomed in view of the red box area in the left panel. Red arrow points to the region of PSM merging. The surgery ablation of pNC usually does not completely remove all NC progenitors, thus restoration of NC further posterior is usually observed.

(E) Joined PSM formed large axial somites posterior to the pNC ablation site. Right panel is a zoomed in view of the red box area in the left panel. Here PSM becomes longer than NC. Note that the NT still co-elongated with the PSM.

(F) Joined PSM on the dorsal side at the pNT ablation site (arrow). Ventral view shows an undamaged NC through the ablation site. Dorsal view show joint somites forming at the NT gap. In this case PSM becomes longer than NT while NC still co-elongated with PSM. Scale bar: 500μm.

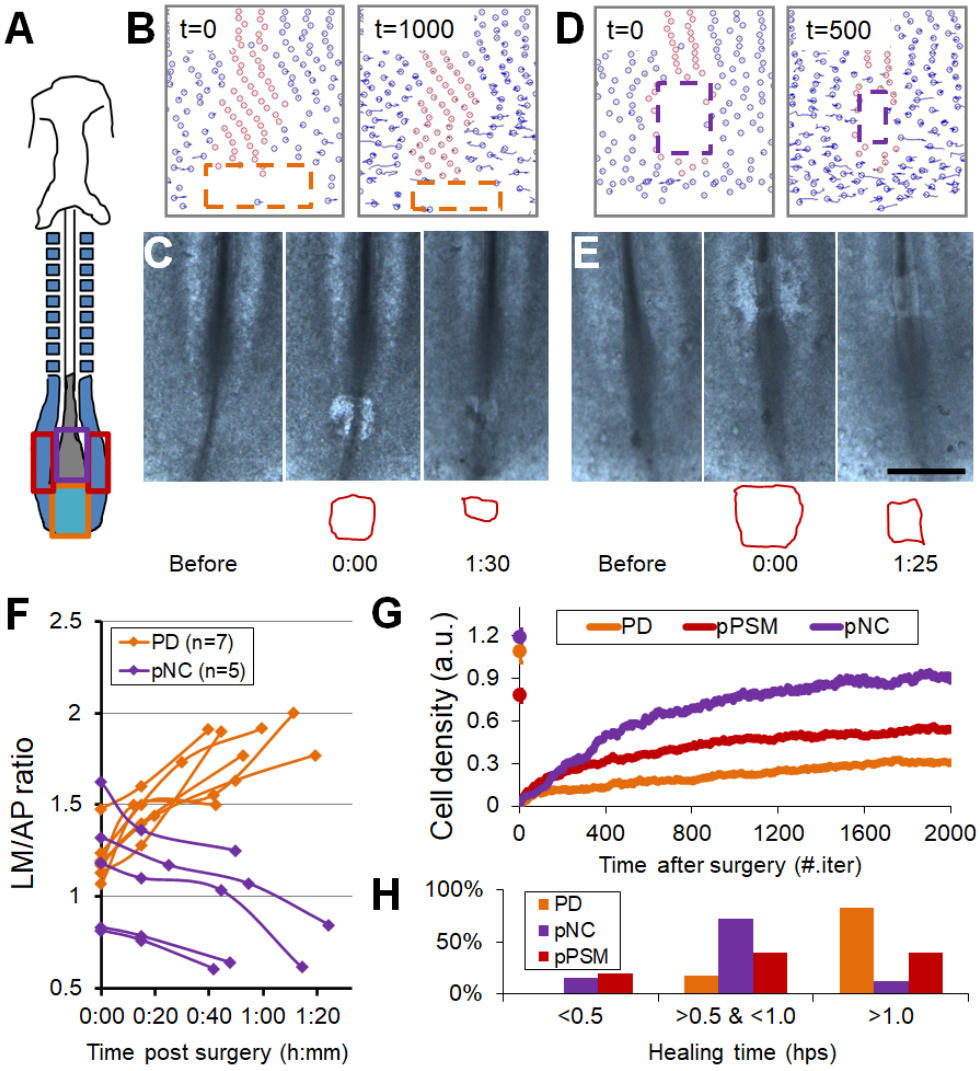

Figure S7. Model predictions of tissue mechanical dynamics, related to Figure 7

(A) Schematic of surgery sites on the embryo corresponding to areas in the model.

(B,D) Simulations of wound closure in response to ablation of PD and pNC. Time indicates number of iterations post-ablation.

(C,E) Closure of rectangle wounds introduced on embryos as shown in (B) and (D), respectively. Red contours outline the shape of the openings. Note that these closing dynamics are much faster than when there is a gel implant. Scale bar: 500μm.

(F) Summary of wound aspect ratio change. The ratios are plotted as LM over AP lengths, indicating spatially differential tissue forces.

(G) Simulated cell density recovery (an approximate measure of wound closure) after cell deletion in the same area. Curves show the average of 30 simulations in each case. Markers ±SD at time 0 indicate cell density before surgery. pNC area is predicted to have the fastest recovery.

(H) Time of complete wound closure by ablated tissues. PD n=17, pNC n=25, pPSM n=15. The majority of pNC wounds close under 1 hps, while the majority of PD wounds remain open.